© 2014. Published by The Company of Biologists Ltd | Development (2014) 141, 3143-3152 doi:10.1242/dev.106989

RESEARCH ARTICLE

STEM CELLS AND REGENERATION

Tcf3 expression marks both stem and progenitor cells in multiple epithelia

Jeffrey M. Howard[1,2,3], Justine M. Nuguid[1,4], Diana Ngole[1] and Hoang Nguyen[1,3,5,6,7,*]

ABSTRACT

The *Lef/Tcf*-family transcription factor *Tcf3* has important roles in development, stem cell function and malignancy. Previous gain- and loss-of-function studies have suggested that *Tcf3* is a mediator of self-renewal and an undifferentiated state in stem and progenitor cells in skin, but little is known of its role in other postnatal tissues. Here, we explore the distribution and behavior of *Tcf3*-expressing cells in several adult tissues using a novel *Tcf3-CreER* knock-in mouse model. By lineage tracing in dorsal skin, we verify that *Tcf3*-expressing cells in the hair follicle bulge are self-renewing stem cells with multilineage potential. We then demonstrate, for the first time, the presence of *Tcf3*-expressing cells in the basal layer of several other stratified epithelia, including the paw skin, tongue and esophagus. By lineage tracing, we demonstrate that the *Tcf3*-expressing population in these tissues includes persistent stem cells, transient progenitors and cells undergoing active differentiation. Our observations here suggest that the role of *Tcf3* in cell-fate decision is more complex than previously appreciated and is highly dependent on cellular context.

KEY WORDS: Tcf transcription factors, Transcription factor 7-like 1 protein, Adult stem cells, Lineage tracing, Mouse

INTRODUCTION

Tcf3 (also known as Tcf7-like 1 or *Tcf7l1*) is a member of the *Lef/Tcf* family, a group of transcription factors with important roles in development, stem cell homeostasis and malignancy. *Tcf3* is a crucial regulator of embryonic stem cell function, where it acts as an inhibitory regulator of the *Oct/Sox/Nanog* pluripotency circuit (Cole et al., 2008; Pereira et al., 2006; Yi et al., 2008, 2011). *Tcf3* also plays a key role in patterning and cell fate specification during early embryonic development (Cole et al., 2008; Dorsky et al., 2003; Houston et al., 2002; Kim et al., 2000; Merrill et al., 2004; Pereira et al., 2006; Yi et al., 2008, 2011). Later in development, *Tcf3* is involved in maintenance and specification of progenitor cells in the central nervous system (Kim and Dorsky, 2011; Kim et al., 2011). Emerging evidence also implicates *Tcf3* in the pathogenesis of several types of human cancer (Ben-Porath et al., 2008; Cole et al., 2008; Pereira et al., 2006; Slyper et al., 2012; Yi et al., 2008, 2011).

[1]Stem Cells and Regenerative Medicine (STaR) Center, Baylor College of Medicine, One Baylor Plaza, Houston, TX 77030, USA. [2]Medical Scientist Training Program, Baylor College of Medicine, One Baylor Plaza, Houston, TX 77030, USA. [3]Program in Translational Biology and Molecular Medicine, Baylor College of Medicine, One Baylor Plaza, Houston, TX 77030, USA. [4]School of Medicine, Southern Illinois University, PO Box 19620, Springfield, IL 62794, USA. [5]Department of Molecular and Cellular Biology, Baylor College of Medicine, One Baylor Plaza, Houston, TX 77030, USA. [6]Department of Dermatology, Baylor College of Medicine, One Baylor Plaza, Houston, TX 77030, USA. [7]Dan L. Duncan Cancer Center, Baylor College of Medicine, One Baylor Plaza, Houston, TX 77030, USA.

*Author for correspondence (hoangn@bcm.edu)

Received 31 December 2013; Accepted 26 June 2014

In the mammalian skin, *Tcf3* is expressed throughout the primordial epithelium during development (Merrill et al., 2004; Nguyen et al., 2006), and in the adult skin it is expressed in the hair follicle bulge, a known stem cell niche (DasGupta and Fuchs, 1999; Merrill et al., 2001). Forced overexpression of *Tcf3* in neonatal mouse skin blocks normal epithelial differentiation and causes epithelial cells to assume an undifferentiated, progenitor-like transcriptional state (Merrill et al., 2001; Nguyen et al., 2006). Conversely, deletion of both *Tcf3* and its closely related paralogue *Tcf4* in developing skin produces an epithelial 'burnout' phenotype, with transient hyperproliferation followed by a failure of long-term self-renewal (Nguyen et al., 2009). Based on these observations, *Tcf3* has been presumed to act as a key mediator of a self-renewing undifferentiated state in skin stem cells. Despite considerable interest in the role of *Tcf3* in stem cell homeostasis and malignancy, however, very little is known of its expression or function in normal adult tissues. Based on its importance in development and the results of our gain- and loss-of-function studies in skin, we hypothesized that *Tcf3* might serve as a general regulator of stem cell function in adult tissues. In the present study, we set out to explore this hypothesis by examining the distribution and behavior of *Tcf3*-expressing cells *in vivo*.

RESULTS

The *Tcf3-2A-eGFP-2A-CreER^{T2}* mouse is a faithful, tightly regulated reporter of *Tcf3* expression *in vivo*

We began by examining the expression pattern of *Tcf3* in adult skin at different stages of the hair cycle. In telogen (resting-phase) skin, Tcf3 protein was detected throughout the hair follicle (HF) bulge, consistent with previous reports (Fig. 1A) (DasGupta and Fuchs, 1999; Merrill et al., 2001). During the anagen (growth) phase, *Tcf3* expression levels were markedly increased in the HF bulge, and still higher levels were noted in cells of the outer root sheath (ORS) (Fig. 1B,C). In the bulb of the growing hair, there was a sharply defined separation between *Tcf3*-positive non-proliferating cells in the ORS and *Lef1*-positive highly proliferative cells in the transit-amplifying hair matrix (Fig. 1D,E).

To determine whether *Tcf3* is a stem cell marker, we sought to observe the fate of *Tcf3*-expressing cells *in vivo* using *Cre/loxP*-based lineage tracing. We generated a knock-in mouse line, *Tcf3-2A-eGFP-2A-CreER^{T2}* (hereafter *Tcf3^{GC}*), in which *eGFP* and *CreER^{T2}* reporter genes were appended to the 3′ end of the native *Tcf3* open reading frame (ORF) using viral 2A 'self-processing' peptides (Fig. 1F) (Szymczak et al., 2004). This strategy was designed to preserve all endogenous regulatory elements and to maintain a functional *Tcf3* ORF. Generation of the *Tcf3* knock-in mouse is described in the methods in the supplementary materials. Targeting of the knock-in construct (supplementary material Fig. S1A) was verified by Southern blotting (supplementary material Fig. S1B); subsequent genotyping was performed by PCR (supplementary material Fig. S1C). In subsequent crosses, heterozygous (*Tcf3$^{GC/+}$*) and homozygous

Development (2014) 141, 3143-3152 doi:10.1242/dev.106989

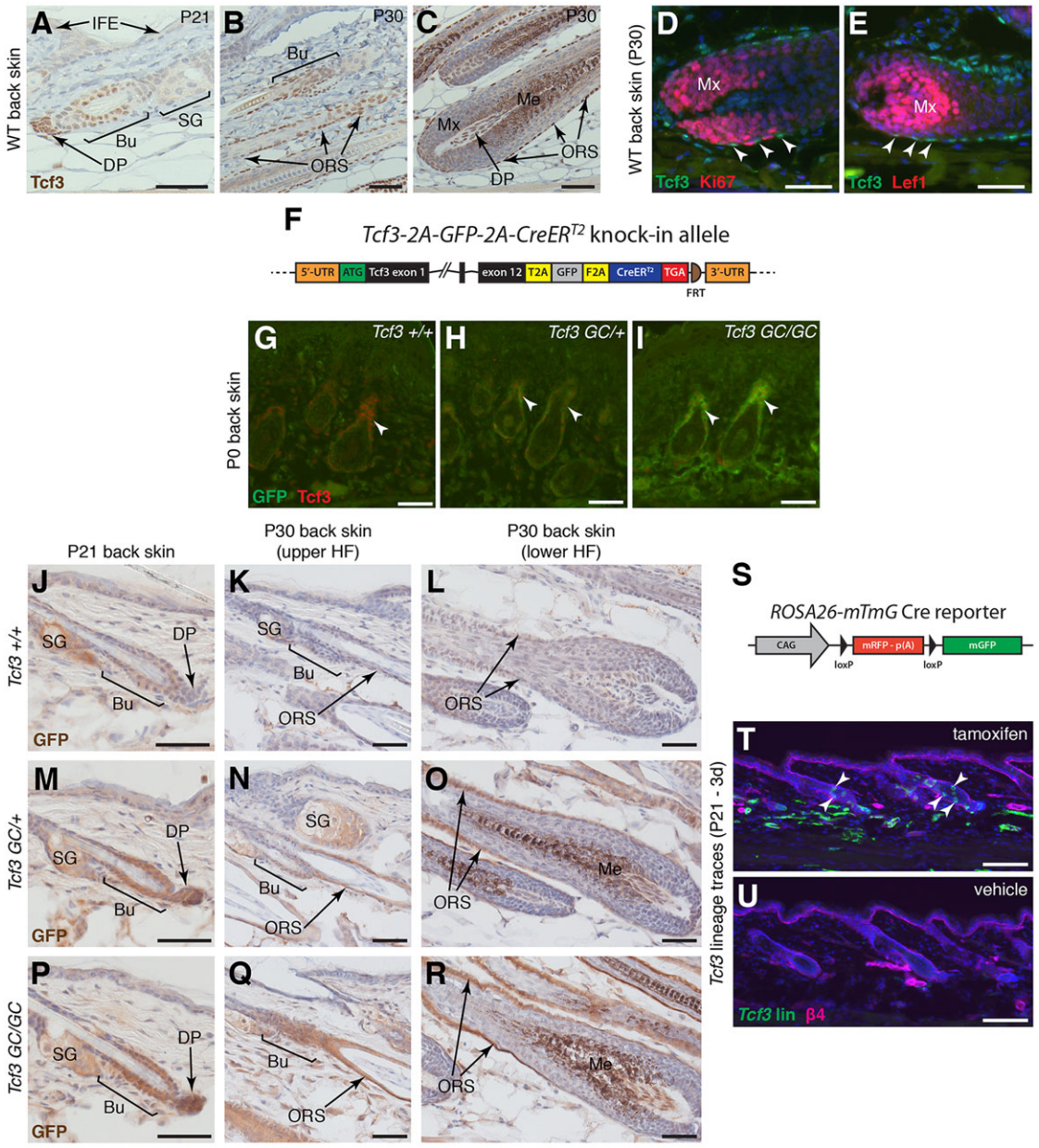

Fig. 1. The *Tcf3-2A-eGFP-2A-CreER^{T2}* mouse is a faithful, tightly regulated reporter of *Tcf3* expression *in vivo*. (A-C) Tcf3 immunohistochemistry in wild-type mouse dorsal skin. (A) In the telogen (resting) phase, *Tcf3* is expressed in the hair follicle bulge (Bu) and dermal papilla (DP), and is absent from the sebaceous gland (SG) and interfollicular epidermis (IFE). (B,C) During anagen, *Tcf3* expression is upregulated in the bulge and is expanded into the outer root sheath (ORS) of the growing hair, but is absent from the transit-amplifying cells of the matrix (Mx). Me, endogenous melanin pigmentation. (D,E) Immunofluorescent co-staining for Tcf3 and either Ki67 (B) or Lef1 (C) in wild-type anagen-phase skin. There is a clear division between *Tcf3*-expressing, non-proliferating ORS cells and *Lef1*-expressing, highly proliferative matrix cells. (F) Schematic of the *Tcf3-2A-eGFP-2A-CreER^{T2}* ('*Tcf3 GC*') knock-in allele. (G-I) Immunofluorescent co-staining for Tcf3 and GFP in neonatal knock-in and wild-type back skin. As expected, GFP colocalizes with Tcf3 in the developing hair follicles (arrowheads). (J-R) Immunohistochemical staining for GFP in *Tcf3$^{+/+}$* (J-L), *$^{GC/+}$* (M-O) and *$^{GC/GC}$* (P-R) adult mouse skin in telogen and anagen phases of the hair cycle. GFP expression is observed in the hair follicle bulge (Bu), dermal papilla (DP) and outer root sheath (ORS), mirroring endogenous *Tcf3* expression (compare A-C). SG, sebaceous gland (with nonspecific staining); Me, endogenous melanin. (S) Schematic of the *ROSA26-mTmG* Cre reporter allele used for lineage tracing. (T,U) Three days after treatment of *Tcf3$^{GC/+}$; ROSA26$^{mTmG/+}$* mice with tamoxifen, individual *Tcf3*-lineage (*Tcf3* lin) mGFP(+) cells are seen in the hair follicle bulge (arrowheads), as well as in various cell types within the dermis including blood vessels (T). No leaky Cre activity is observed in vehicle-treated controls (U). β4, β4 integrin. Scale bars: 100 µm in T,U; 50 µm in A-E,G-R.

(*Tcf3$^{GC/GC}$*) knock-in mice were born in Mendelian ratios. They were viable, fertile, and bore no obvious phenotype (supplementary material Fig. S1D), suggesting that the knock-in allele preserved normal *Tcf3* gene function. In isolated skin keratinocytes from newborn mice, Tcf3 protein was detected at near wild-type levels in both heterozygous and homozygous knock-in animals, with no evidence of 'read-through' (incomplete processing) of the 2A peptides (supplementary material Fig. S1E). The knock-in GFP reporter was too dim for direct microscopy or cell-sorting applications, but it was easily detectable by immunostaining and colocalized with endogenous Tcf3 in neonatal back skins (Fig. 1G-I). In adult knock-in mice, the expression pattern of the knock-in GFP marker mirrored that

Development (2014) 141, 3143-3152 doi:10.1242/dev.106989

of Tcf3 in both telogen- and anagen-phase back skins (Fig. 1J-R) as well as the other epithelial tissues we subsequently studied (supplementary material Fig. S1F-N; compare Fig. 4A,B, Fig. 5A,B and Fig. 6A,B).

For lineage-tracing experiments, we crossed *Tcf3*^{GC} with *ROSA26*^{mTmG} mice (Muzumdar et al., 2007), which express membrane-bound GFP (mGFP) following Cre activation (Fig. 1S). By treating *Tcf3*$^{GC/+}$; *ROSA26*$^{mTmG/+}$ mice with tamoxifen, we were able to mark *Tcf3*-expressing cells with the genetically encoded *mGFP* label, allowing us to monitor the fate of *Tcf3*-expressing cells and their progeny *in vivo*. After inducing these mice with tamoxifen, we observed mGFP(+) cells in *Tcf3*-expressing cell types throughout the skin, including the hair follicle bulge (Fig. 1T, arrowheads). CreER activity was very tightly regulated, with not a single mGFP(+) cell appearing in vehicle-treated control mice in any of the tissues we studied (n>20 across all timepoints) (Fig. 1U; supplementary material Fig. S2P,R,T). Based on these observations, we concluded that our novel *Tcf3*^{GC} allele is a faithful, tightly regulated reporter of endogenous *Tcf3* expression *in vivo*.

Tcf3 expression marks lineage-restricted hair follicle stem cells in the murine dorsal skin

Using the *Tcf3*^{GC}/*ROSA26*^{mTmG} lineage-tracing system, we first examined the fate of *Tcf3*-expressing cells in murine dorsal skin. We treated *Tcf3*$^{GC/+}$; *ROSA26*$^{mTmG/+}$ mice (n=5-7 per timepoint) with tamoxifen on postnatal days 21 and 22, during the first telogen (resting) phase of the hair cycle. Three days after treatment, we observed labeled cells in the HF bulge and hair germ (Fig. 2A,B). We also noted *Tcf3* reporter activity in various cell types within the dermis, including (notably) the dermal papilla (Fig. 2B) and dermal blood vessels (supplementary material Fig. S2A,B).

During the succeeding anagen phase, labeled *Tcf3*-lineage clones expanded and incorporated into all differentiated lineages of the hair shaft (Fig. 2C-H). Six months after induction, persistent clones were seen in both telogen- and anagen-phase follicles (Fig. 2I-K). Similar results were obtained when lineage traces were initiated during the second postnatal telogen (supplementary material Fig. S2C-E). There was a moderate, nonsignificant reduction (68.4±3.7% of initial, mean±s.d.; P=0.42, Mann–Whitney U-test) in the number of labeled follicles from 3 days to 6 months post induction (supplementary material Fig. S2F), consistent with a model in which most or all HF bulge cells possess stem cell potential but are occasionally lost from the stem cell niche, as previously described by others (Hsu et al., 2011; Zhang et al., 2010).

We became curious about the fate of *Tcf3*-expressing cells during anagen, when *Tcf3* is highly expressed throughout the outer root sheath (ORS) of the growing hair. We treated *Tcf3*$^{GC/+}$; *ROSA26*$^{mTmG/+}$ mice (n=4-6) with tamoxifen during anagen (typically at P30) and sacrificed them 3 days or 4 weeks after induction. Even with a single dose of tamoxifen, nearly all hair follicles contained multiple mGFP(+) clones in the ORS 3 days after induction (Fig. 2L), some of which were captured in transition between the ORS and matrix and thus appeared to be committing to terminal differentiation (supplementary material Fig. S2G). Labeled cells were also observed in the HF bulge at a relatively low frequency (16.5±7.2%, mean±s.d.) (Fig. 2M). Four weeks after induction, when mice had returned to telogen, a much larger proportion (70.3±16.6%, mean±s.d.; P=0.0095, Mann–Whitney U-test) of HFs contained one or more labeled cells in the bulge region, implying that *Tcf3*-lineage cells in the ORS survive the catagen (regression) phase to re-incorporate into the newly formed bulge (Fig. 2N,O). Cells within the new bulge have been shown to differ in their functions: cells in the outer layer of the bulge are true stem cells, while inner-layer cells serve a regulatory function and lack stem cell potential (Hsu et al., 2011). In our experiment, ORS-derived *Tcf3*-lineage cells incorporated into both populations in roughly equal proportions [62.6±0.2% of labeled bulges contained mGFP(+) cells in the outer bulge] (Fig. 2O), indicating that *Tcf3*-expressing ORS cells are capable of assuming either fate.

In the course of these experiments, the *Tcf3* lineage was never observed in the upper portions of the hair follicle, the sebaceous gland (SG) or the interfollicular epidermis (IFE). Previous reports have indicated that HF bulge-derived cells can incorporate into the IFE during epithelial wound repair (Brownell et al., 2011; Ito et al., 2005; Page et al., 2013). We examined this behavior in *Tcf3*-expressing cells by labeling HF bulge cells at higher frequency by injecting *Tcf3*$^{GC/GC}$ homozygous lineage-tracing mice with tamoxifen (either two or three doses) starting at P21 and subjecting them to full-thickness wounding 5 days after the last dose. One week after wounding, mGFP(+) cells were observed migrating out of wound-adjacent hair follicles and incorporating into the wound epithelium, generally in the suprabasal layers (Fig. 3A,B, arrowheads). There was a trend towards non-persistence of these cells over time, however, with the majority of cells being lost from the wound epithelium by 3-4 weeks post wounding (Fig. 3C). Some persistent clones were observed, frequently in close association with wound-edge hair follicles (Fig. 3D,E). The total number of persistent cells 4 weeks post wounding was 22.8±10.4% (mean±s.d.) of the initial timepoint (this result approached but did not reach significance at P=0.09, Mann–Whitney U-test) (Fig. 3F). This observation is consistent with prior studies that have shown a long-term persistence rate of ∼20% of bulge-derived cells (Page et al., 2013). Bulge-derived *Tcf3*-lineage clones formed radial tracks within the wound epithelium similar to those previously described for *K15*, *K19* and *Lgr5* (Fig. 3G,H).

Tcf3 expression marks both persistent and non-persistent cells in hairless paw skin

Because the *Tcf3* lineage was strictly excluded from the stratified IFE in normal dorsal skin, we asked whether *Tcf3* might be expressed in the plantar paw skin, which, like human palmar skin, lacks hair follicles. *Tcf3* was expressed in the basal epithelium of the plantar paw skin; however, rather than being confined to a rare subpopulation of stem cells, it was expressed ubiquitously throughout the basal layer (Fig. 4A,B), most highly in the thick skin of the digital pads (Fig. 4C).

To determine the stem cell potential of *Tcf3*-expressing cells in the paw skin, we administered tamoxifen to *Tcf3*$^{GC/+}$; *ROSA26*$^{mTmG/+}$ mice at P21 and P22, and examined the skin at various timepoints thereafter (n=5-8 mice per timepoint). Three days after induction, we observed small clones of one or two cells in the basal layer in a pattern, consistent with our Tcf3 antibody staining (Fig. 4D). By 4 weeks post induction, the clones had expanded to occupy all layers of the stratified epithelium (Fig. 4I-L), and full-thickness clones continued to be seen at subsequent timepoints (Fig. 4E-H). A proportion (although not a majority) of these clones persisted for ≥6 months *in vivo*, suggesting that the cells in which they arose possessed stem cell potential. We also noted extensive labeling of hair follicles in the neighboring haired skin that, as in the dorsal skin, was confined to the hair follicle (Fig. 4M).

Tcf3 expression marks both persistent and non-persistent cells in the esophageal mucosa

We then inquired whether *Tcf3* might be expressed in nonkeratinized as well as in keratinized epithelia. A survey of reporter activity revealed *Tcf3* expression in the esophageal and

Development (2014) 141, 3143-3152 doi:10.1242/dev.106989

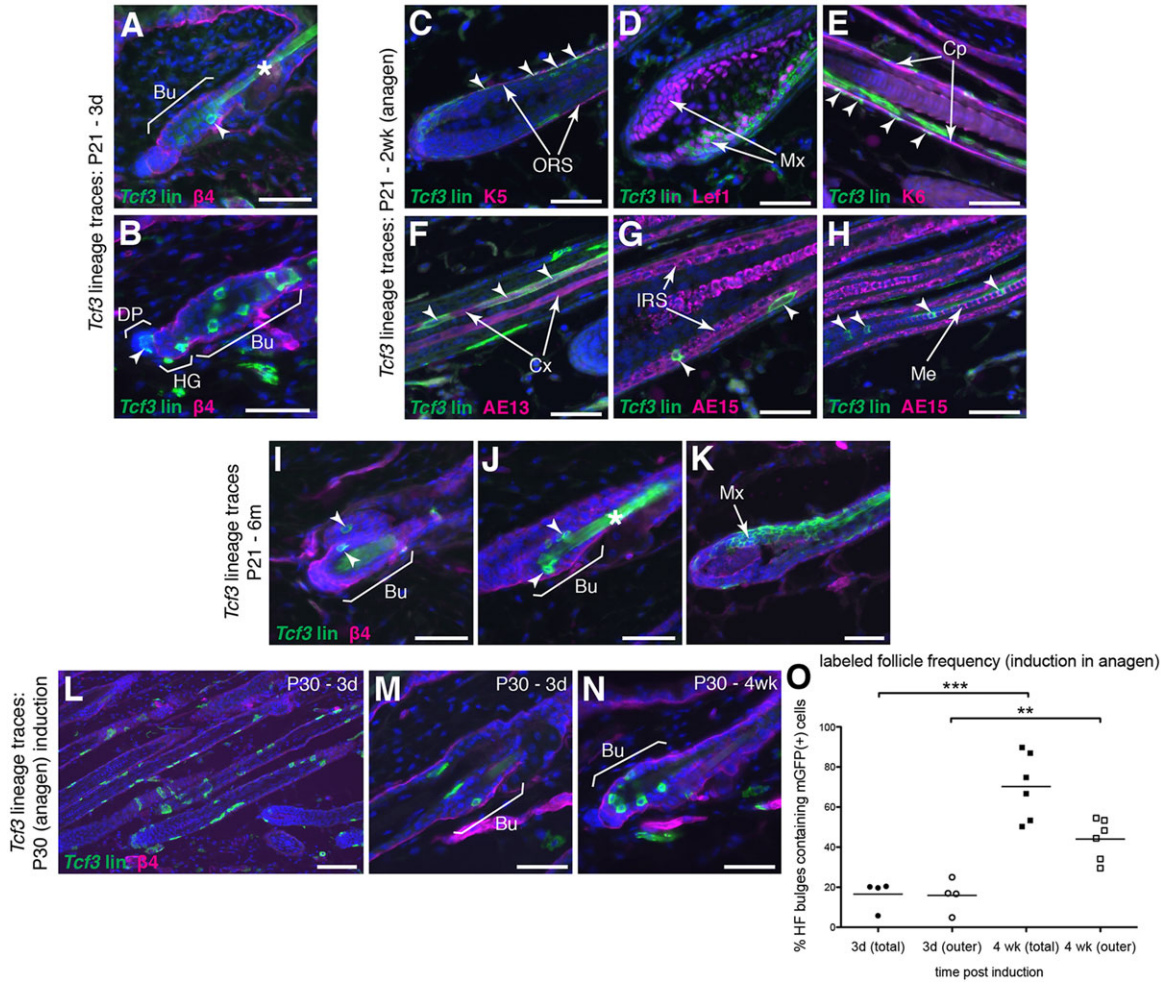

Fig. 2. *Tcf3* expression marks hair follicle stem cells in murine dorsal skin. (A-K) Lineage traces in *Tcf3*-expressing hair follicle bulge cells. *Tcf3*$^{GC/+}$; *ROSA26*$^{mTmG/+}$ mice were treated with tamoxifen at P21 and P22 and sacrificed 3 days to 6 months after induction. (A,B) Individual *Tcf3*-lineage (*Tcf3* lin) cells in the HF bulge (Bu) (A, arrowhead), hair germ (HG) and dermal papilla (DP) (B, arrowhead) 3 days after induction. Asterisk indicates hair shaft autofluorescence. (C-H) Two weeks after induction, *Tcf3*-lineage cells (arrowheads) are seen in the keratin 5 (K5)-positive outer root sheath (ORS) (C), Lef1-positive transit-amplifying matrix cells (Mx) (D) and all differentiated lineages of the hair shaft. Hair shaft lineage markers: companion layer (Cp) and keratin 6 (K6) (E); cortex (Cx) and hair cortex cytokeratin (AE13) (F); inner root sheath (IRS) and medulla (Me), trichohyalin (AE15) (G,H). (I-K) Six months after treatment, persistent clones of single and multiple cells are detected in the bulge (Bu) of both telogen- (I) and anagen-phase (J) hair follicles (arrowheads). In anagen skin, mGFP(+) clones expand and incorporate into growing hair shafts via the transit-amplifying hair matrix (Mx) (K). (L-O) Lineage traces in *Tcf3*-expressing cells during anagen. *Tcf3*$^{GC/+}$; *ROSA26*$^{mTmG/+}$ mice were treated with tamoxifen during full anagen (~P30) and sacrificed 3 days or 4 weeks after induction. (L,M) Three days after induction, numerous *Tcf3*-lineage clones are seen in the outer root sheath of nearly all follicles (L); a minority of follicles also show labeling in the bulge (Bu) (M). (N) Four weeks after induction, when mice have re-entered telogen, most bulges contain mGFP(+) cells. (O) Quantification of the proportion of HFs containing mGFP(+) cells in the bulge region 3 days and 4 weeks after lineage-tracing induction during anagen. The analysis was performed in two ways: first, counting follicles with labeled cells in any portion of the bulge (dark circles/squares); second, counting only follicles containing cells in the outer layer of the bulge (open circles/squares). Only a minority of bulge regions (16.5±7.2% for total bulge, 15.9±8.3% for outer bulge) contain mGFP(+) cells at the initial timepoint. The proportion rises to 70.2±16.6% (total bulges) or 44.0±10.3% (outer bulges) after follicles have returned to telogen (all percentages mean±s.d.; P=0.0095 for both comparisons, Mann–Whitney U-test). Data points represent percentage of HF bulge regions containing mGFP(+) cells in individual mice; bars indicate mean. β4, β4 integrin. Scale bars: 100 μm in L; 50 μm in A-K,M,N.

lingual mucosa (discussed below), but not in more distal regions of the GI tract. In the esophagus, as in the paw skin, *Tcf3* was expressed throughout the epithelial basal layer (Fig. 5A,B) and in some suprabasal cells within the lower granular layer (supplementary material Fig. S3A).

To assess the stem cell potential of *Tcf3*-expressing basal cells, we performed lineage-tracing experiments as described for the paw skin, inducing mice (n=6-8 per timepoint) with tamoxifen at P21 and P22 and sacrificing at various timepoints thereafter. Three days after tamoxifen treatment, clones of 1-2 mGFP(+) cells were detected in both the epithelial basal layer (Fig. 5C) and in isolated suprabasal cells (supplementary material Fig. S3C), consistent with the expression pattern seen in immunostaining. Over time, the labeled basal cells gave rise to columns of differentiated cells occupying the full thickness of the epithelium (Fig. 5D-J). As in the paw skin, some clones persisted *in vivo* for ≥6 months (Fig. 5H), indicating that the cells in which they arose were self-renewing stem cells. As in the paw skin, however, the majority of *Tcf3*-lineage clones failed to persist over time.

The majority of *Tcf3*-lineage clones are lost from paw skin and esophageal mucosa over time

Previous studies have examined the self-renewal dynamics of the esophagus and paw skin; it was concluded that both tissues followed

Development (2014) 141, 3143-3152 doi:10.1242/dev.106989

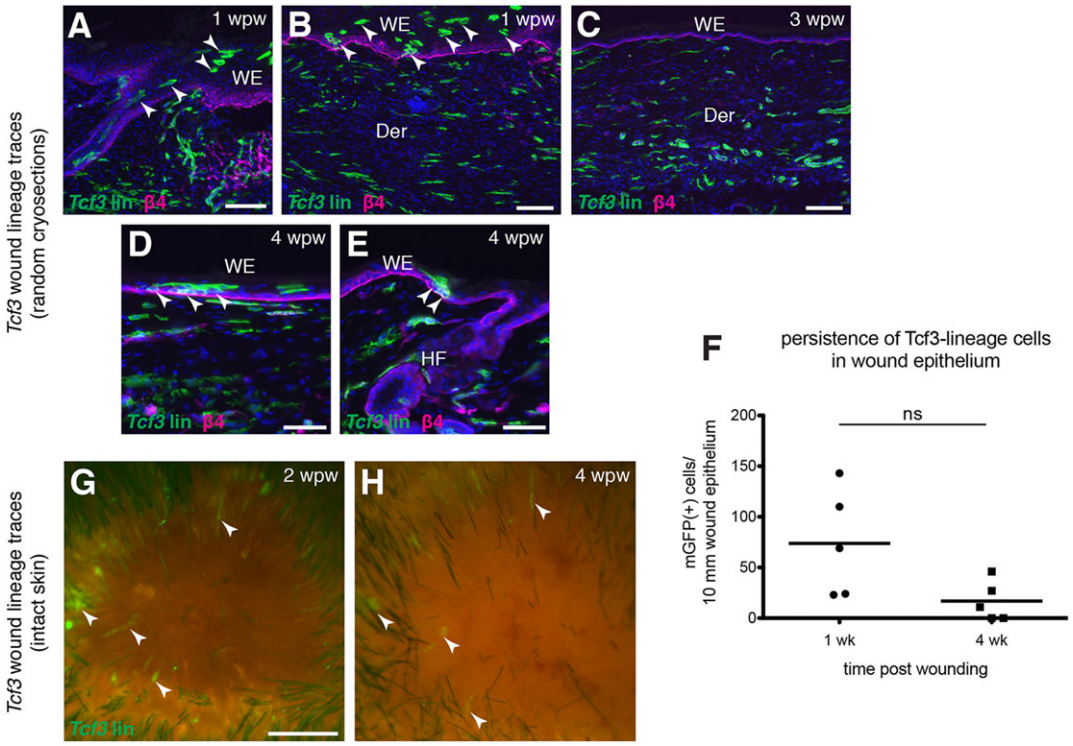

Fig. 3. *Tcf3*-expressing hair follicle bulge cells contribute to wound repair of the interfollicular epithelium, but most fail to persist long term. *Tcf3* lineage-tracing experiments in wounded epithelia. *Tcf3*$^{GC/GC}$; *ROSA26*$^{mTmG/+}$ mice were treated with tamoxifen at P21, P23 and P25, wounded at P30, and sacrificed 1-4 weeks after wounding. (A-E) Random cryosections of wound epithelium 1-4 weeks after wounding. (A) One week after wounding, *Tcf3*-lineage (*Tcf3* lin) cells are observed migrating out of wound-adjacent hair follicles and incorporating into the wound epithelium (WE). (B) *Tcf3*-lineage cells (arrowheads) in the wound epithelium are primarily seen in the suprabasal layers. Numerous *Tcf3*-lineage cells are also seen in the wound dermis (Der). (C) By 3-4 weeks post wounding, the majority of *Tcf3*-lineage cells are lost from the wound epithelium but persist in the dermis. (D,E) A subset of *Tcf3*-lineage cells (arrowheads) does persist in the wound epithelium, frequently (E) associated with wound-adjacent hair follicles (HF). (F) Quantification of *Tcf3*-lineage clones in wound epithelium 1 and 4 weeks after wounding. Dots indicate number of mGFP(+) cells per 10 mm of wound epithelium in random cryosections at each timepoint; bars indicate mean. There is a trend towards cell loss over time, with only a minority (22.8±10.4%, mean±s.d.) of labeled cells persisting for at least 4 weeks (P=0.093, Mann–Whitney U-test). (G,H) Images of intact wound epithelium in *Tcf3* lineage-tracing mice 2 (G) and 4 (H) weeks after wounding. Rare clones of mGFP(+) cells (arrowheads) are grossly visible in the wound epithelium, many of which are absent at the later timepoint. *Tcf3* lin, *Tcf3* lineage; β4, β4 integrin. Scale bars: 100 μm in A-C; 50 μm in D,E; 1 mm in G,H.

a neutral-competition homeostasis in which all basal cells have equivalent potential for long-term persistence and there is no defined subpopulation of stem cells (Doupé et al., 2012; Lim et al., 2013). Conversely, other studies have suggested the existence of a stem cell hierarchy in the interfollicular back skin (Mascré et al., 2012). Although the experiments described here were not intended to address mechanisms of homeostasis, we became curious about whether our results were compatible with a neutral competition model in which all *Tcf3*-expressing basal cells possess an equal chance of long-term persistence. For both tissues, we quantitated the number of mGFP(+) clones, the number of labeled basal cells within each clone and the total number of mGFP(+) basal cells in multiple random cryosections at each timepoint.

In both tissues, the majority of *Tcf3*-lineage clones were lost over time, with only 9.9±8.7% (paw skin) or 17.0±6.6% (esophagus) of initial clones persisting at 6 months post-induction (both mean±s.d., both P<0.001, Dunn's multiple comparison test) (supplementary material Fig. S4A,D). In both tissues, the surviving clones expanded laterally through the basal layer over time (P<0.0001 for both tissues, Kruskal–Wallis test) (supplementary material Fig. S4B,E). A key prediction of the neutral competition model is that the total number of labeled basal cells remains constant over time, as the loss of some clones is exactly balanced by the expansion of surviving clones. Interestingly, there appeared to be a general decline in the total number of basal cells over time in both tissues, though this only reached statistical significance when comparing the 3-day and 6-month timepoints (P<0.01 for paw skin, P<0.05 for esophagus, Dunn's multiple comparison test) (supplementary material Fig. S4C,F). Although this result could be interpreted to mean that *Tcf3*-expressing cells possess a slightly reduced capacity for long-term (>6 months) self-renewal, it is also possible that it may simply reflect under-sampling of clones at the later timepoints due to the low initial labeling frequency. Further experiments are necessary to clarify this issue, but in any event these data are incompatible with a model in which *Tcf3* expression labels a master stem cell population that is preferentially fated to long-term survival.

Tcf3 expression marks both stem and committed cells in the lingual epithelium

The murine lingual epithelium is considerably more complex than the esophagus and possesses specialized appendages incorporating various differentiated cell types. The most numerous of these are the filliform papillae (FPs), hook-shaped structures that occupy the majority of the dorsal epithelial surface. Each FP consists of distinct anterior and posterior elements that are themselves distinct from the epithelium of the interpapillary pits (IPPs) (Hume and Potten, 1976). Recent reports have described a rare population of *Bmi1*-expressing epithelial stem cells that self-renew for extended periods

Development (2014) 141, 3143-3152 doi:10.1242/dev.106989

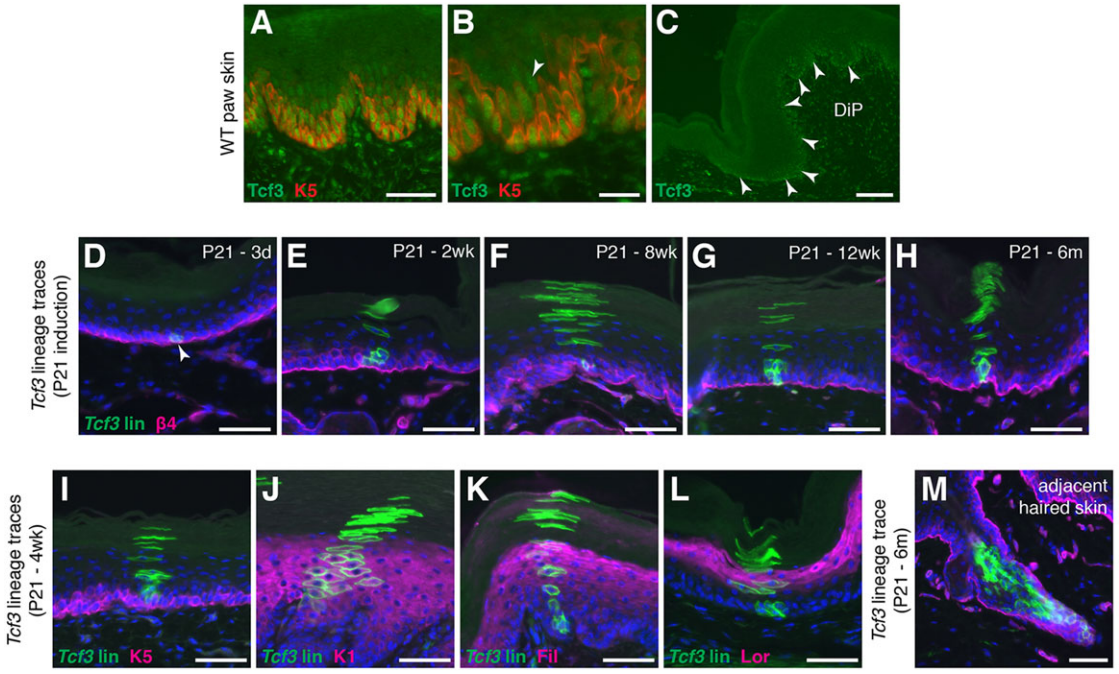

Fig. 4. *Tcf3* expression marks stem and progenitor cells in unhaired paw skin. (A-C) Immunofluorescent co-staining for Tcf3 and basal marker keratin 5 (K5) in wild-type plantar paw skin. (A,B) *Tcf3* expression is seen throughout the basal layer of the stratified paw skin and, at lower levels, in occasional suprabasal cells (B, arrowhead). (C) *Tcf3* is most highly expressed in the thick skin overlying the digital pads (DiP) (arrowheads). (D-L) Lineage tracing in paw skins of $Tcf3^{GCI/+}$; $ROSA26^{mTmG/+}$ mice. Mice were treated with tamoxifen at P21 and P22 and sacrificed 3 days to 6 months after induction. (D) Three days post induction, single *Tcf3*-lineage (*Tcf3* lin) cells are labeled in the basal layer. β4, β4 integrin. (E-H) Over time, mGFP(+) clones gave rise to columns of differentiated cells occupying the full thickness of the epithelium; some clones persisted for at least 6 months *in vivo* (H). (I-L) Epithelial layers and markers: basal layer, keratin 5 (K5) (I); spinous layer, keratin 1 (K1) (J) and filaggrin (Fil) (K); granular layer, loricrin (Lor) (L). (M) Extensive labeling was observed in hair follicles in adjacent haired paw skin. As in the dorsal skin, these were confined to the HF and never extended into the IFE. Scale bars: 20 µm in B; 100 µm in C; 50 µm in A,D-M.

and give rise to all differentiated lineages of the tongue *in vivo* (Tanaka et al., 2013).

We first examined the expression pattern of *Tcf3* in the lingual epithelium by immunostaining. *Tcf3* was expressed at varying levels throughout the epithelial basal layer, most highly in the base of the interpapillary pits (Fig. 6A,B), and also at moderate levels in some suprabasal cells (supplementary material Fig. S3B). This contrasted sharply with the previously described stem cell marker *Bmi1*, which occurred at a frequency of ~1 cell/IPP (Tanaka et al., 2013). To examine the relationship between the *Tcf3* and *Bmi1* populations, we performed short-term (2 day) lineage traces in $Bmi1^{CreER/+}$; $ROSA26^{mTmG/+}$ mice (Sangiorgi and Capecchi, 2008).

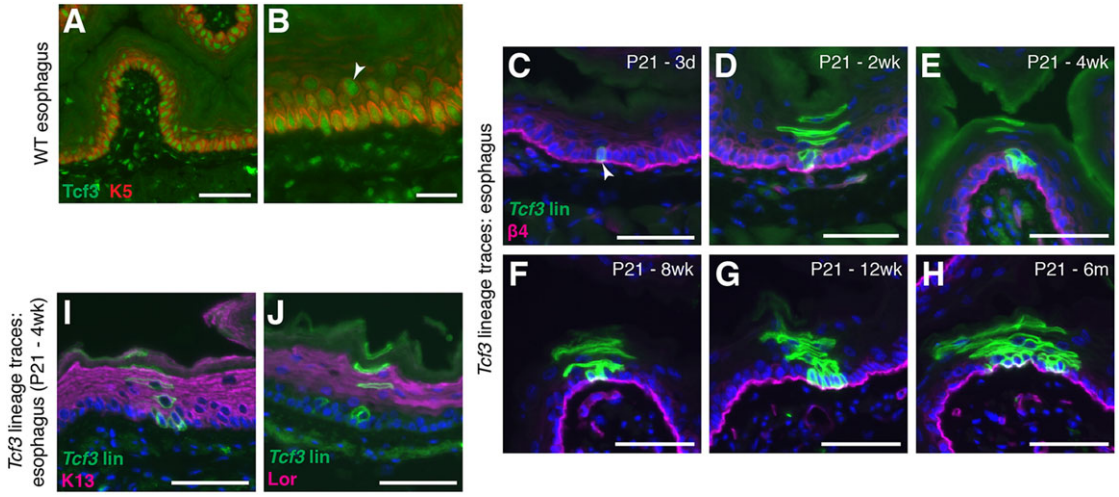

Fig. 5. *Tcf3* expression marks stem and progenitor cells in esophageal mucosa. (A,B) Immunofluorescent co-staining for Tcf3 and basal marker keratin 5 (K5) in wild-type esophageal mucosa. *Tcf3* is expressed throughout the basal layer and in some suprabasal cells (B, arrowhead). (C-J) Lineage tracing in esophageal mucosa of $Tcf3^{GCI/+}$; $ROSA26^{mTmG/+}$ mice. Mice were treated with tamoxifen at P21/22 and sacrificed 3 days to 6 months after induction. (C) Three days post induction, small clones of 1-3 *Tcf3*-lineage (*Tcf3* lin) cells were seen, primarily in the epithelial basal layer (arrowhead). β4, β4 integrin. (D-J) Over time, mGFP(+) clones formed columns of differentiated cells occupying the full thickness of the epithelium; some clones persisted for at least 6 months *in vivo* (H). Epithelial markers: suprabasal cells, keratin 13 (K13) (I); granular layer (Lor) (J). Scale bars: 20 µm in B; 50 µm in A,C-J.

Development (2014) 141, 3143-3152 doi:10.1242/dev.106989

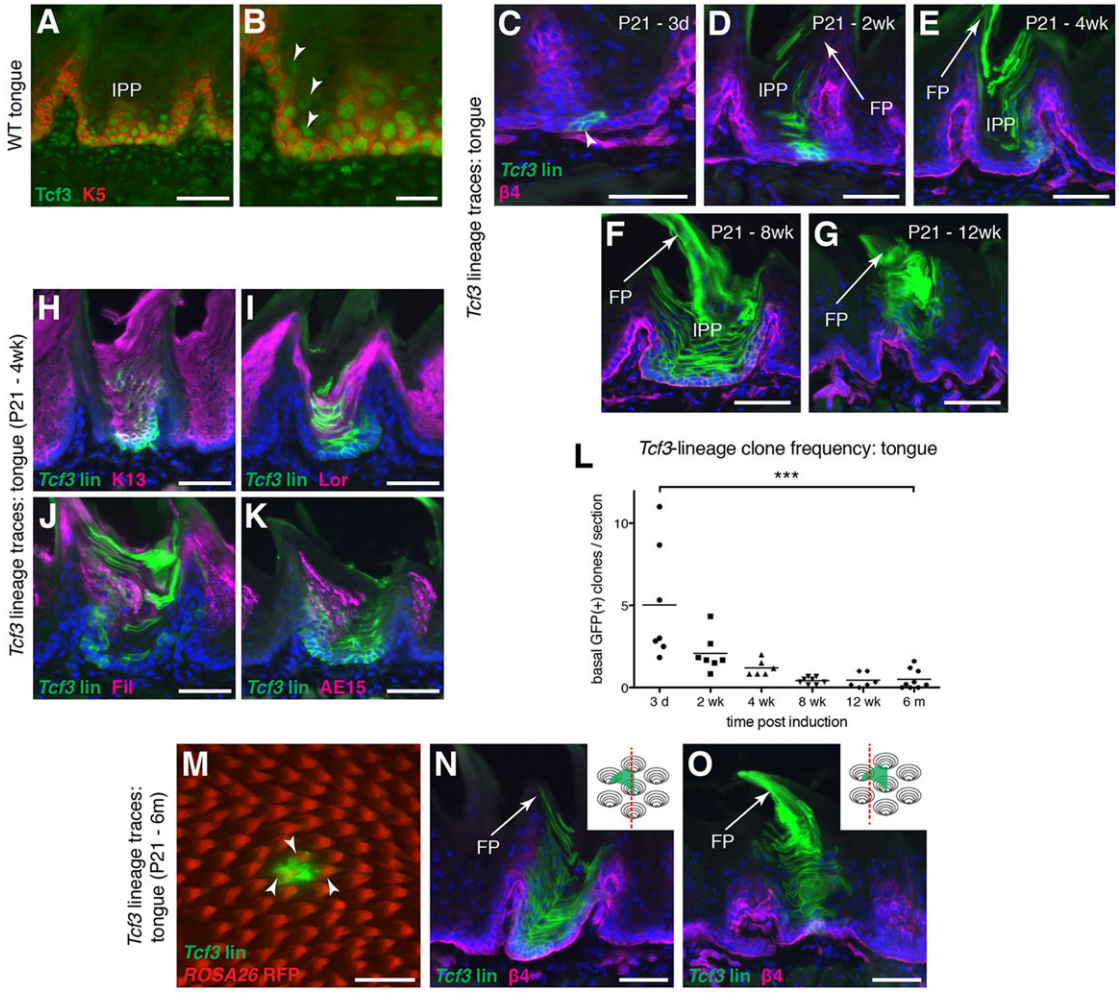

Fig. 6. *Tcf3* expression marks stem and progenitor cells in lingual mucosa. (A,B) Immunofluorescent co-staining for Tcf3 and basal marker keratin 5 (K5) in wild-type dorsal tongue. *Tcf3* expression is seen throughout the basal layer and at lower levels and in some suprabasal cells (B, arrowheads). (C-K) Lineage tracing in lingual epithelium of $Tcf3^{GCI/+}$; $ROSA26^{mTmGI/+}$ mice. Mice were treated with tamoxifen at P21 and P22 and sacrificed 3 days to 6 months after induction. (C) Three days after induction, clones of 2-5 mGFP(+) cells were seen in the epithelial basal layer (arrowhead). (D-K) Labeled clones expanded over time and incorporated into both filliform papilla (FP) and interpapillary pit (IPP) lineages. Cell type markers: interpapillary epithelium, keratin 13 (K13) (H); granular layer, loricrin (Lor) (I); filliform papillae, filaggrin (Fil) (J) and trichohyalin (AE15) (K). (L) The overwhelming majority of *Tcf3*-lineage clones were lost from the lingual epithelium over time, most within the first few weeks after induction. Clone frequency at 6 months post induction was only 10.0±5.1% (mean±s.d.) of the initial timepoint (P<0.001, Dunn's multiple comparison test). Dots indicate number of mGFP(+) clones per sagittal section of dorsal tongue in individual mice; bars indicate mean. (M-O) The dorsal surface of the tongue is covered by a dense layer of hook-shaped filliform papillae (FPs) in staggered rows. FPs are separated by interpapillary pits (IPPs) containing a distinct interpapillary epithelium (IPE). Long-term persistent clones occupied the entirety of a single interpapillary pit and incorporated into regions of the three or four neighboring filliform papillae, similar to previously described *Bmi1*-lineage clones (Tanaka et al., 2013). (M) Whole-mount image of intact dorsal epithelium from a P21 to 6 months lineage tracing tongue. Individual FPs are visible as triangular structures expressing the constitutive *ROSA26-mT* label. An individual mGFP(+) clone is seen, occupying a single IPP and contributing to each of the three neighboring FPs (arrowheads). (N,O) Sections cut through different planes of mGFP(+) clones in P21 to 6 months lineage-tracing tongue specimen, illustrating contribution of labeled cells to the anterior and posterior (N) or lateral (O) compartments of neighboring FPs. Insets represent a top-down schematic view of the dorsal tongue, showing the location of the section (red dashed line) within the labeled clone (green triangle) and relative to the neighboring FPs (conical structures). β4, β4 integrin. Scale bars: 20 µm in B; 200 µm in M; 50 µm in A,C-K,N,O.

The *Bmi1*-expressing population was identified at a frequency of ~1 cell/IPP, consistent with the observations of Tanaka and colleagues. Interestingly, some of these cells expressed *Tcf3* at levels similar to neighboring basal cells (supplementary material Fig. S5A, arrowheads), whereas others expressed little to no *Tcf3* (supplementary material Fig. S5B, arrowheads), suggesting that expression of the two factors is not directly related. Similarly, there was little correlation between *Tcf3* expression and proliferative status, with cells variously expressing Tcf3 or Ki67, or both, at varying levels (supplementary material Fig. S5C).

To assess the stem cell potential of *Tcf3*-expressing cells in the lingual epithelium, we performed lineage-tracing experiments according to the same protocol used for the esophagus and paw skin (n=7-9 mice per timepoint). Three days after induction, we observed small clones of ~2-4 labeled cells in the basal layer (Fig. 6C), as well as solitary labeled suprabasal cells (supplementary material Fig. S3D). Over the subsequent weeks and months, the basal clones continued to expand (Fig. 6D-G). Immunostaining at the 4-week timepoint demonstrated incorporation of *Tcf3*-lineage cells into multiple differentiated cell lineages in the tongue, including both the interpapillary epithelium (labeled by K13 and loricrin) and the filliform papillae (labeled by filaggrin and trichohyalin) (Fig. 6H-K). As in the esophagus and paw skin, the overwhelming majority of *Tcf3*-lineage cells failed to persist over time, suggesting that the

Development (2014) 141, 3143-3152 doi:10.1242/dev.106989

majority of the *Tcf3*-expressing population is not fated to long-term persistence: the clone frequency at 6 months was only ~10% of the initial timepoint (Fig. 6L). A minority of *Tcf3*-lineage clones did persist for ≥6 months *in vivo* and thus presumably arose from true stem cells.

Interestingly, those rare clones that did persist to the 6-month timepoint nearly always occupied the entirety of an interpapillary pit (IPP) and contributed to part of each of the neighboring 3-4 filliform papillae (Fig. 6M-O). This observation suggests that IPPs are separately maintained units of self-renewal and that each FP is maintained as a mosaic with contributions from at least three distinct individual stem cells, consistent with the prior results of Tanaka et al. (2013). Given the relatively low number of clones observed at this timepoint, however, we cannot rule out the possibility that there is some sharing of cells between adjacent IPPs, especially over a longer (>6 months) timeframe.

DISCUSSION

Numerous studies employing label-retention and genetic fate-mapping techniques have demonstrated that hair follicle bulge cells are self-renewing stem cells that are responsible for maintenance of the hair follicle through its cycles of growth, regression and rest, but do not contribute significantly to the IFE during normal homeostasis (Cotsarelis et al., 1990; Ito et al., 2005; Jaks et al., 2008; Morris et al., 2004; Tumbar et al., 2004). Our results from lineage tracing of telogen-phase skin are consistent with this established consensus. There is some disagreement among previous studies regarding the capacity of HF bulge cells to contribute to the sebaceous gland; fate-mapping experiments have demonstrated a contribution of *K15*-lineage cells to the SG during normal homeostasis (Morris et al., 2004; Petersson et al., 2011), whereas *Lgr5*-lineage cells do not appear to incorporate into the SG, at least in the absence of injury (Jaks et al., 2008). Consistent with the previous *Lgr5* study, we never observed labeled cells in the SG in the course of our experiments, suggesting that the *Tcf3* lineage is normally excluded from the SG. However, given the relatively low labeling efficiency achieved in our experiments, we cannot rule out the possibility that cells expressing low levels of *Tcf3* do contribute to the SG under some circumstances.

Our wound-repair experiments are also consistent with prior observations that HF bulge cells are mobilized into the IFE during epidermal wound repair but mostly (~60-90%) fail to persist over time (Ito et al., 2005; Page et al., 2013). Given our comparatively low labeling frequency and the low persistence of *Tcf3*-lineage cells in the wound epithelium, however, we cannot rule out the possibility that *Tcf3* expression preferentially marks a subset of bulge cells with a reduced capacity to assume the IFE SC identity. There is some precedent for the idea that subsets of bulge cells differ in their capacity to persist in IFE, as the majority of persistent cells appear to arise from a *Gli1*-expressing subpopulation in the upper bulge (Brownell et al., 2011).

Of particular interest are our results from fate mapping of *Tcf3*-expressing cells in the anagen-phase ORS, which appear to include a mixture of both stem and progenitor cells. At the initial timepoint, clones were observed in transition between the ORS and matrix, implying that they were committing to differentiation. However, a proportion of labeled ORS cells did survive beyond the end of anagen to re-incorporate into both the inner and outer layers of the newly formed HF bulge. These observations independently confirm prior studies that used label-retention methods to demonstrate the persistence of a defined subset of ORS cells (Hsu et al., 2011); they also suggest that *Tcf3* expression is not exclusive to stem cells, at least during the anagen phase. It is interesting to note that, in both telogen- and anagen-induction lineage traces, the behavior of *Tcf3*-expressing cells closely resembled that previously described for *Lgr5*-expressing cells (Jaks et al., 2008), and it seems likely that – at least in the dorsal skin – the two factors label the same population of cells.

Having observed that *Tcf3*-lineage cells were strictly excluded from the stratified IFE in normal dorsal skin, we were surprised to observe that *Tcf3* was broadly expressed in the basal layer of several other stratified epithelia (paw skin, esophagus and tongue). In all three cases, a proportion of *Tcf3*-lineage clones persisted for extended periods of time *in vivo* and thus originated in self-renewing stem cells, but the majority of *Tcf3*-lineage clones failed to persist and were lost over time. Both the broad expression of *Tcf3* and non-persistence of *Tcf3*-expressing cells were surprising in light of our initial hypothesis that *Tcf3* expression would label defined, self-renewing stem cell populations.

The contrast with our expectations was especially marked in the tongue, where the majority of labeled clones were lost within the first few weeks after lineage tracing induction, implying that the cells in which they arose were short-lived committed progenitors. Over time, the *Tcf3* lineage-tracing results converged with that previously seen for *Bmi1*-expressing SCs, with persistent *Tcf3*-lineage clones occupying the entirety of an IPP and contributing to the three neighboring filliform papillae. Importantly, the relative survival of *Bmi1*-lineage clones was not quantified in the previous study (Tanaka et al., 2013), and it is therefore uncertain whether the *Bmi1* population represent classical stem cells at the apex of a stem-progenitor hierarchy or, alternately, if the *Bmi1* population is in competitive homeostasis with other populations of self-renewing cells. In the former case, the persistent *Tcf3*-lineage clones in our study would presumably have originated in *Bmi1*-expressing cells. Although we cannot distinguish between these possibilities, we do conclude that *Tcf3* expression in the lingual epithelium encompasses a wide range of stem, progenitor and committed cells.

The esophageal mucosa and plantar paw skin have recently been characterized as following a neutral-competition model of homeostasis, in which all basal cells have an equal probability of long-term persistence and undergo stochastic cell-fate decisions (Doupé et al., 2012; Lim et al., 2013). According to such a model, there is no stem-progenitor hierarchy and all basal cells are arguably 'stem cells'. Progressive clone loss is an inherent feature of such systems and the observed non-persistence of *Tcf3*-lineage clones over time would thus be a predictable outcome. Even under the loose definition of 'stemness' posited by the neutral competition model, however, *Tcf3* expression is not restricted to stem cells, as it is also observed in differentiating suprabasal cells that are rapidly lost from the epithelium.

Interestingly, quantitation of our lineage-tracing data suggests a decline in the total number of labeled basal cells over time (supplementary material Fig. S4), implying that *Tcf3* expression labels a subset of basal cells with reduced capacity for long-term persistence. This would suggest at least a partial stem-progenitor hierarchy in these tissues and would thus conflict with the established neutral competition model. It is important to note, however, that these findings were derived from a *post hoc* analysis of experiments that were not originally designed to address this issue. There are also numerous differences between our methods and those of previous groups; for example, the previous work of Lim et al. (2013) analyzed only the region of the plantar epithelium lacking eccrine sweat glands (which, notably, expresses *Tcf3* at very low levels), whereas our analysis included the entire plantar

Development (2014) 141, 3143-3152 doi:10.1242/dev.106989

paw skin. Although further experiments are clearly called for in order to evaluate this fascinating discrepancy, it does not fundamentally alter our conclusion that *Tcf3* is not a sole determinant of stem cell identity.

Based on the expression pattern of *Tcf3* and our previous gain- and loss-of-function results (Merrill et al., 2001; Nguyen et al., 2006, 2009), we anticipated that *Tcf3* expression would serve as a marker of defined, self-renewing tissue stem cell populations in various tissues. Although the behavior of *Tcf3*-expressing hair follicle bulge cells was generally consistent with this hypothesis, we were surprised to observe that in the tissues we studied, *Tcf3* was expressed not only in long-term persistent stem cells but also in short-lived progenitors and, in some cases, in cells undergoing early differentiation. These findings suggest that physiological *Tcf3* expression alone is insufficient to maintain a cell in an undifferentiated self-renewing state *in vivo* and imply a more complex role for *Tcf3* in epithelial homeostasis than previously appreciated. Recent studies in the hair follicle have demonstrated that *Tcf3* functions as part of a complex 'rheostat' that, in competition with the canonical Wnt/β-catenin pathway, determines stem cell behavior (Lien et al., 2014). It seems likely that a similar mechanism, in which *Tcf3* is a contributor to but not the sole determinant of cell fate, holds in the other tissues we studied. It is also important to note emerging evidence that *Tcf3* plays a role in processes beyond stem-cell fate decisions: recent studies by our group have demonstrated that *Tcf3* acts as a key regulator of cell migration within the wound-repair microenvironment (Miao et al., 2014). This is particularly pertinent in light of our incidental observation here that *Tcf3* is expressed in a variety of non-epithelial cell types, sometimes at very high levels.

Given our findings and the observations discussed above, it is likely that *Tcf3* has varying, context-dependent functions in developing and adult tissues, and in different cell types within the adult organism, probably due to the presence or absence of additional co-factors such as Groucho/TLE proteins. Findings concerning the functions of *Tcf3* in development might therefore not be generalizable to normal adult tissues or to malignancy. Our results here call for further experiments to clarify the exact functions of *Tcf3* in normal and disease biology, with special attention to the cellular context in which *Tcf3* expression occurs.

MATERIALS AND METHODS

Mice and experiments

All experiments were approved by the Baylor College of Medicine (BCM) Institutional Animal Care and Use Committee (IACUC). *ROSA26-mTmG* (Muzumdar et al., 2007) and *Bmi1-CreER* (Sangiorgi and Capecchi, 2008) mice have been described elsewhere and were obtained from The Jackson Laboratory. *Tcf3* knock-in mice were generated by standard gene targeting techniques described in the methods in the supplementary material. Polymerase chain reaction (PCR) primers used in cloning and genotyping are listed in supplementary material Table S1.

Lineage-tracing experiments

For lineage-tracing experiments, $Tcf3^{GC/+}$; $ROSA26^{mTmG/+}$ mice were treated with tamoxifen (unless otherwise noted, two doses of 40 mg/ml tamoxifen in 85% corn oil/15% ethanol, 5 µl/g body weight on days P21 and P22). For wounding experiments, mice were subjected to 8 mm full-thickness punch wounds on the midline dorsal skin 5 days after induction. For quantitative comparisons of clone size and frequency over time, clones [defined as clusters of one or more closely associated mGFP(+) cells including at least one basal cell] and the number of basal cells per clone were counted in random non-serial 8 µm cryosections (five or six sagittal sections for tongue and paw skin, 15-45 transverse sections for esophagus). Graphing and statistical analysis was performed using GraphPad Prism (GraphPad Software). Statistical comparisons were performed using nonparametric tests (Mann–Whitney *U*-test or Kruskal–Wallis test with Dunn's multiple comparison post-test, as appropriate). Values of $P<0.05$ were deemed significant.

Immunofluorescence, immunohistochemistry and western blotting

For detection of the ROSA26-mGFP lineage-tracing reporter, tissues were prefixed in 1-4% paraformaldehyde prior to processing for frozen sections. Frozen sections and immunofluorescent staining, and image acquisition, as well as western blots of neonatal keratinocytes, were performed as described previously (Leishman et al., 2013). Nuclear counterstaining was performed with Hoechst 33342 (Life Technologies) (blue channel where shown). Immunohistochemical detection of Tcf3 (in formalin-fixed, paraffin-embedded sections) or of GFP (in fixed-frozen sections) was performed using the Vectastain Elite ABC system (Vector Labs), in some cases with heat-induced epitope retrieval in 10 mM sodium citrate (pH 6.0). Antibodies used in immunofluorescence, immunohistochemistry and western blotting are listed in supplementary material Table S2.

Acknowledgements

We thank everyone involved in the preparation and publication of this work, including T. M. Shaver, and Drs H. Dierick, M. A. Goodell, M. C. V. Ngo, M. Rendl and J. Rosen for their critical reading of the manuscript. We also thank I. Lorenzo, Drs A. Rodriguez and M. Justice of the Mouse Embryonic Stem Cell Core Facility, and Dr F. DeMayo of the Genetically Engineered Mouse Shared Resource, both BCM facilities, for their technical contributions and expertise.

Competing interests

The authors declare no competing financial interests.

Author contributions

J.M.H. designed and constructed the knock-in mouse and designed and performed all experiments and data analysis. J.M.N. and D.N. assisted with experiments and animal husbandry. H.N. designed experiments and supervised the project. J.M.H. and H.N. prepared the manuscript.

Funding

The project was supported by the National Institutes of Health (NIH) [NIH/NIAMS R01-AR059122] and by the Cancer Prevention and Research Institute of Texas (CPRIT) [RP110153] (both to H.N.). J.M.H. was supported in part by training grants [NIH T32-HL092332-07 (to Dr H. Heslop) and CPRIT RP101499 (to Dr J. Rosen)]. J.M.N. was supported in part by the Mentored Professional Enrichment Experience (MPEE) program at Southern Illinois University School of Medicine. The Mouse Embryonic Stem Cell Core Facility and the Genetically Engineered Mouse Shared Resource were supported in part by the NIH [NIH/NCI P30 CA125123 to the Dan L. Duncan Cancer Center at BCM]. Deposited in PMC for release after 12 months.

Supplementary material

Supplementary material available online at
http://dev.biologists.org/lookup/suppl/doi:10.1242/dev.106989/-/DC1

References

Ben-Porath, I., Thomson, M. W., Carey, V. J., Ge, R., Bell, G. W., Regev, A. and Weinberg, R. A. (2008). An embryonic stem cell-like gene expression signature in poorly differentiated aggressive human tumors. *Nat. Genet.* **40**, 499-507.

Brownell, I., Guevara, E., Bai, C. B., Loomis, C. A. and Joyner, A. L. (2011). Nerve-derived sonic hedgehog defines a niche for hair follicle stem cells capable of becoming epidermal stem cells. *Cell Stem Cell* **8**, 552-565.

Cole, M. F., Johnstone, S. E., Newman, J. J., Kagey, M. H. and Young, R. A. (2008). Tcf3 is an integral component of the core regulatory circuitry of embryonic stem cells. *Genes Dev.* **22**, 746-755.

Cotsarelis, G., Sun, T.-T. and Lavker, R. M. (1990). Label-retaining cells reside in the bulge area of pilosebaceous unit: implications for follicular stem cells, hair cycle, and skin carcinogenesis. *Cell* **61**, 1329-1337.

DasGupta, R. and Fuchs, E. (1999). Multiple roles for activated LEF/TCF transcription complexes during hair follicle development and differentiation. *Development* **126**, 4557-4568.

Dorsky, R. I., Itoh, M., Moon, R. T. and Chitnis, A. (2003). Two tcf3 genes cooperate to pattern the zebrafish brain. *Development* **130**, 1937-1947.

Doupé, D. P., Alcolea, M. P., Roshan, A., Zhang, G., Klein, A. M., Simons, B. D. and Jones, P. H. (2012). A single progenitor population switches behavior to maintain and repair esophageal epithelium. *Science* **337**, 1091-1093.

Development (2014) 141, 3143-3152 doi:10.1242/dev.106989

Houston, D. W., Kofron, M., Resnik, E., Langland, R., Destree, O., Wylie, C. and Heasman, J. (2002). Repression of organizer genes in dorsal and ventral Xenopus cells mediated by maternal XTcf3. *Development* **129**, 4015-4025.

Hsu, Y.-C., Pasolli, H. A. and Fuchs, E. (2011). Dynamics between stem cells, niche, and progeny in the hair follicle. *Cell* **144**, 92-105.

Hume, W. J. and Potten, C. S. (1976). The ordered columnar structure of mouse filiform papillae. *J. Cell Sci.* **22**, 149-160.

Ito, M., Liu, Y., Yang, Z., Nguyen, J., Liang, F., Morris, R. J. and Cotsarelis, G. (2005). Stem cells in the hair follicle bulge contribute to wound repair but not to homeostasis of the epidermis. *Nat. Med.* **11**, 1351-1354.

Jaks, V., Barker, N., Kasper, M., van Es, J. H., Snippert, H. J., Clevers, H. and Toftgård, R. (2008). Lgr5 marks cycling, yet long-lived, hair follicle stem cells. *Nat. Genet.* **40**, 1291-1299.

Kim, H.-S. and Dorsky, R. I. (2011). Tcf7l1 is required for spinal cord progenitor maintenance. *Dev. Dyn.* **240**, 2256-2264.

Kim, C.-H., Oda, T., Itoh, M., Jiang, D., Artinger, K. B., Chandrasekharappa, S. C., Driever, W. and Chitnis, A. B. (2000). Repressor activity of Headless/Tcf3 is essential for vertebrate head formation. *Nature* **407**, 913-916.

Kim, S., Chung, A.-Y., Kim, D., Kim, Y.-S., Kim, H.-S., Kwon, H.-W., Huh, T.-L. and Park, H.-C. (2011). Tcf3 function is required for the inhibition of oligodendroglial fate specification in the spinal cord of zebrafish embryos. *Mol. Cells* **32**, 383-388.

Leishman, E., Howard, J. M., Garcia, G. E., Miao, Q., Ku, A. T., Dekker, J. D., Tucker, H. and Nguyen, H. (2013). Foxp1 maintains hair follicle stem cell quiescence through regulation of Fgf18. *Development* **140**, 3809-3818.

Lien, W.-H., Polak, L., Lin, M., Lay, K., Zheng, D. and Fuchs, E. (2014). In vivo transcriptional governance of hair follicle stem cells by canonical Wnt regulators. *Nat. Cell Biol.* **16**, 179-190.

Lim, X., Tan, S. H., Koh, W. L. C., Chau, R. M. W., Yan, K. S., Kuo, C. J., van Amerongen, R., Klein, A. M. and Nusse, R. (2013). Interfollicular epidermal stem cells self-renew via autocrine Wnt signaling. *Science* **342**, 1226-1230.

Mascré, G., Dekoninck, S., Drogat, B., Youssef, K. K., Brohée, S., Sotiropoulou, P. A., Simons, B. D. and Blanpain, C. (2012). Distinct contribution of stem and progenitor cells to epidermal maintenance. *Nature* **489**, 257-262.

Merrill, B. J., Gat, U., DasGupta, R. and Fuchs, E. (2001). Tcf3 and Lef1 regulate lineage differentiation of multipotent stem cells in skin. *Genes Dev.* **15**, 1688-1705.

Merrill, B. J., Pasolli, H. A., Polak, L., Rendl, M., García-García, M. J., Anderson, K. V. and Fuchs, E. (2004). Tcf3: a transcriptional regulator of axis induction in the early embryo. *Development* **131**, 263-274.

Miao, Q., Ku, A. T., Nishino, Y., Howard, J. M., Rao, A. S., Shaver, T. M., Garcia, G. E., Le, D. N., Karlin, K. L., Westbrook, T. F. et al. (2014). Tcf3 promotes cell migration and wound repair through regulation of lipocalin 2. *Nat. Commun.* **5**, 4088.

Morris, R. J., Liu, Y., Marles, L., Yang, Z., Trempus, C., Li, S., Lin, J. S., Sawicki, J. A. and Cotsarelis, G. (2004). Capturing and profiling adult hair follicle stem cells. *Nat. Biotechnol.* **22**, 411-417.

Muzumdar, M. D., Tasic, B., Miyamichi, K., Li, L. and Luo, L. (2007). A global double-fluorescent Cre reporter mouse. *Genesis* **45**, 593-605.

Nguyen, H., Rendl, M. and Fuchs, E. (2006). Tcf3 governs stem cell features and represses cell fate determination in skin. *Cell* **127**, 171-183.

Nguyen, H., Merrill, B. J., Polak, L., Nikolova, M., Rendl, M., Shaver, T. M., Pasolli, H. A. and Fuchs, E. (2009). Tcf3 and Tcf4 are essential for long-term homeostasis of skin epithelia. *Nat. Genet.* **41**, 1068-1075.

Page, M. E., Lombard, P., Ng, F., Göttgens, B. and Jensen, K. B. (2013). The epidermis comprises autonomous compartments maintained by distinct stem cell populations. *Cell Stem Cell* **13**, 471-482.

Pereira, L., Yi, F. and Merrill, B. J. (2006). Repression of Nanog gene transcription by Tcf3 limits embryonic stem cell self-renewal. *Mol. Cell. Biol.* **26**, 7479-7491.

Petersson, M., Brylka, H., Kraus, A., John, S., Rappl, G., Schettina, P. and Niemann, C. (2011). TCF/Lef1 activity controls establishment of diverse stem and progenitor cell compartments in mouse epidermis. *EMBO J.* **30**, 3004-3018.

Sangiorgi, E. and Capecchi, M. R. (2008). Bmi1 is expressed in vivo in intestinal stem cells. *Nat. Genet.* **40**, 915-920.

Slyper, M., Shahar, A., Bar-Ziv, A., Granit, R. Z., Hamburger, T., Maly, B., Peretz, T. and Ben-Porath, I. (2012). Control of breast cancer growth and initiation by the stem cell-associated transcription factor TCF3. *Cancer Res.* **72**, 5613-5624.

Szymczak, A. L., Workman, C. J., Wang, Y., Vignali, K. M., Dilioglou, S., Vanin, E. F. and Vignali, D. A. A. (2004). Correction of multi-gene deficiency in vivo using a single "self-cleaving" 2A peptide-based retroviral vector. *Nat. Biotechnol.* **22**, 589-594.

Tanaka, T., Komai, Y., Tokuyama, Y., Yanai, H., Ohe, S., Okazaki, K. and Ueno, H. (2013). Identification of stem cells that maintain and regenerate lingual keratinized epithelial cells. *Nat. Cell Biol.* **15**, 511-518.

Tumbar, T., Guasch, G., Greco, V., Blanpain, C., Lowry, W. E., Rendl, M. and Fuchs, E. (2004). Defining the epithelial stem cell niche in skin. *Science* **303**, 359-363.

Yi, F., Pereira, L. and Merrill, B. J. (2008). Tcf3 functions as a steady-state limiter of transcriptional programs of mouse embryonic stem cell self-renewal. *Stem Cells* **26**, 1951-1960.

Yi, F., Pereira, L., Hoffman, J. A., Shy, B. R., Yuen, C. M., Liu, D. R. and Merrill, B. J. (2011). Opposing effects of Tcf3 and Tcf1 control Wnt stimulation of embryonic stem cell self-renewal. *Nat. Cell Biol.* **13**, 762-770.

Zhang, Y. V., White, B. S., Shalloway, D. I. and Tumbar, T. (2010). Stem cell dynamics in mouse hair follicles: a story from cell division counting and single cell lineage tracing. *Cell Cycle* **9**, 1504-1510.

SUPPLEMENTAL MATERIALS AND METHODS

Generation of *Tcf3-2A-eGFP-2A-CreER^{T2}* knock-in mice

To generate *Tcf3* knock-in mice, the targeting construct (Figure S1A) was generated by two-step gap repair recombineering (Lee et al., 2009). First, the *2A-eGFP-2A-CreER^{T2}* fragment was generated by overlap extension PCR in two steps using the primers GFP_T2A_fw, GFP_F2A_rv, Cre_F2A_fw, and Cre_Nhe_Eco_rv with the plasmids pMSCV-IRES-GFP (Addgene #20672, Tannishtha Reya lab) and pCAG-CreER^{T2} (Addgene #14797, Connie Cepko lab) as templates. The resulting fusion product was cloned into plasmid PL451 (Liu et al., 2003) containing a *PGKneo* selection cassette. A *2A-eGFP-2A-CreER^{T2}-PGKneo* fragment was then PCR-amplified with appropriate genomic homology using primers T3KI_cass_fw/rv and recombined into a 129Sv-derived bacterial artificial chromosome (BAC) (Adams et al., 2005) containing the desired portion of the *Tcf3* gene (clone bMQ275e20; obtained from Source BioScience, Nottingham, UK). Finally, the targeting construct and appropriate homology arms were recombined by gap repair into the plasmid PL253, which had been PCR-amplified using primers PL253_genom_L2/R2. The targeting vector was electroporated into AB2.2 mouse embryonic stem cells (ESCs) by the Mouse Embryonic Stem Cell Core Facility at BCM. ESC clones were initially screened by long-range PCR using Crimson LongAmp *Taq* polymerase (New England Biolabs, Ipswich, MA, USA) with primers T3KI_5LR2_fw/rv and T3KI_3LR_fw/rv (data not shown). Targeting was confirmed in selected clones by Southern blot of *Spe*I-digested DNA using probes outside the 3' and 5' homology arms (Figure S1B). Southern blots were performed using the DIG nonisotopic

detection system (Roche Applied Sciences, Indianapolis, IN, USA) according to the manufacturer's instructions; probes were generated using PCR primers T3KI_5SB_fw/rv and T3KI_3SB_fw/rv. Germline transmission in agouti-colored progeny of chimeric mice was verified by Southern blot (data not shown) and subsequent genotyping was performed by PCR using primers Tcf3KI_fw, Tcf3KI_GC_rv, and Tcf3KI_WT_rv (Figure S1C). Mice with germline transmission of the knock-in allele were crossed with *ROSA26-FLPe* mice (Farley et al., 2000) in order to delete the *FRT*-flanked *PGKneo* drug selection cassette (Figure S1A). Primers used in cloning and genotyping are listed in Table S1.

SUPPLEMENTAL REFERENCES

Adams, D. J., Quail, M. A., Cox, T., van der Weyden, L., Gorick, B. D., Su, Q., Chan, W.-I., Davies, R., Bonfield, J. K., Law, F., et al. (2005). A genome-wide, end-sequenced 129Sv BAC library resource for targeting vector construction. *Genomics* **86**, 753–758.

Farley, F. W., Soriano, P., Steffen, L. S. and Dymecki, S. M. (2000). Widespread recombinase expression using FLPeR (flipper) mice. *Genesis* **28**, 106–110.

Lee, S.-C., Wang, W. and Liu, P. (2009). Construction of gene-targeting vectors by recombineering. *Methods Mol. Biol.* **530**, 15–27.

Liu, P., Jenkins, N. A. and Copeland, N. G. (2003). A highly efficient recombineering-based method for generating conditional knockout mutations. *Genome Res.* **13**, 476–484.

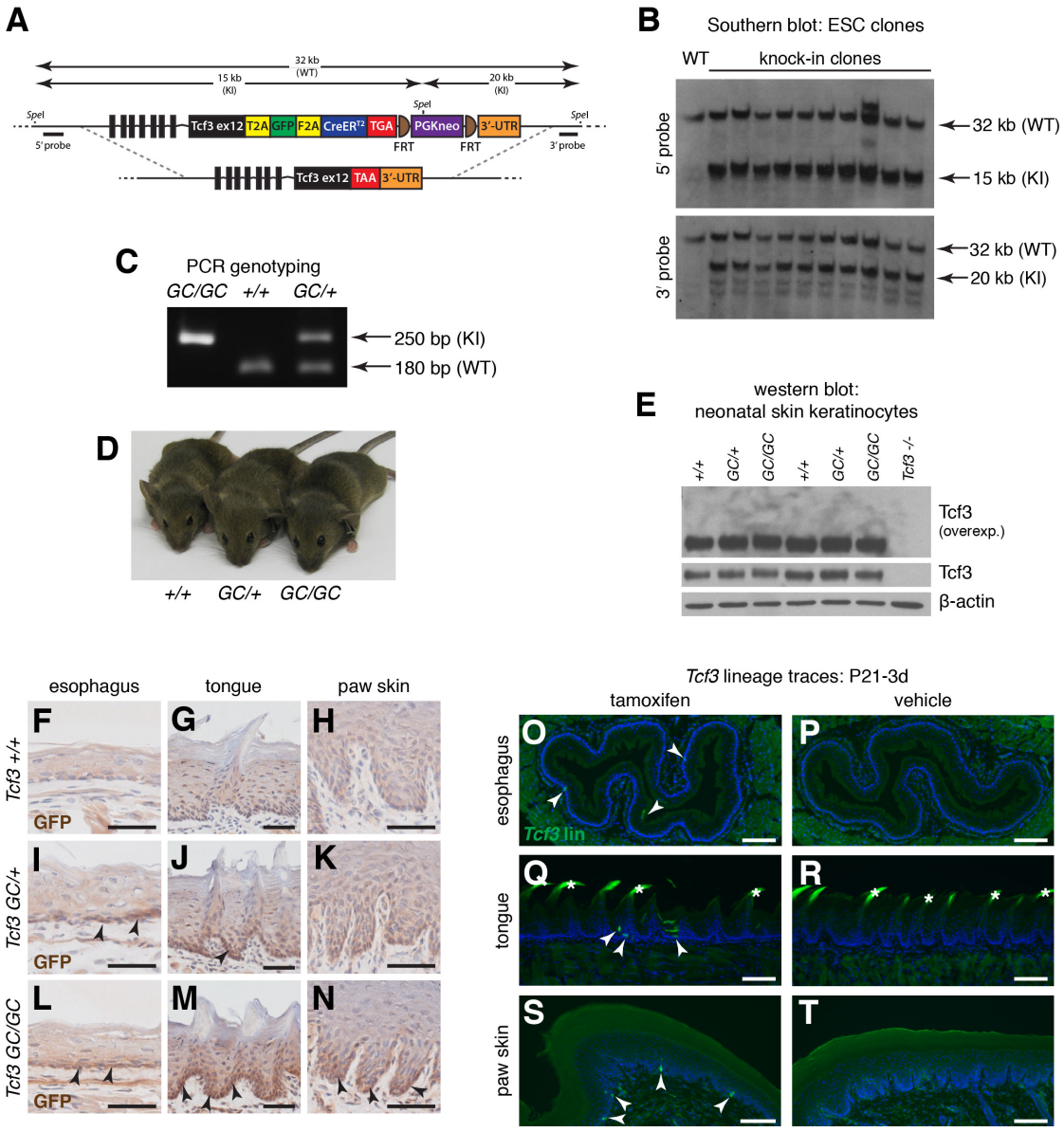

Figure S1. Generation and validation of *Tcf3* knock-in mice.

(**A**) Schematic of *Tcf3* knock-in targeting strategy, showing targeting construct (top) and the targeted region of the wild-type genome (bottom). *Spe*I restriction sites and location of 5' and 3' probes for Southern blotting are shown.

(**B**) Representative example of Southern blot to confirm targeting in ESC clones. *Spe*I-digested genomic DNA was separated on an agarose gel and probed first with the 5' probe, then stripped and re-probed with the 3' probe. One clone (third from right) shows an abnormal double insertion; the others yield the expected bands. WT: control gDNA from wild-type ES cells.

(**C**) Representative results from routine PCR genotyping of *Tcf3* knock-in mice.

(**D**) Representative image of young adult (P50) $Tcf3^{+/+}$, $^{GC/+}$, and $^{GC/GC}$ littermates. Knock-in mice are viable, fertile, and manifest no obvious phenotype.

(**E**) Western blot of Tcf3 expression in neonatal skin keratinocytes from $Tcf3^{+/+}$, $^{GC/+}$, and $^{GC/GC}$ mice. Knock-in mice express Tcf3 at wild-type levels (middle panel). No Tcf3-GFP fusion products are detected even with prolonged exposure (top panel), suggesting minimal "read-through" of the 2A peptides *in vivo*. Far right lane contains protein from $Tcf3^{-/-}$ keratinocytes as a negative control.

(**F-N**) Immunohistochemical staining for GFP in esophagus, tongue, and plantar paw skin of $Tcf3^{+/+}$, $^{GC/+}$, and $^{GC/GC}$ mice. In all three tissues, *Tcf3*-GFP expression is detected in the epithelial basal layer (arrowheads) in a pattern mirroring that of endogenous Tcf3 (compare Figures 3A-C, 4A-D).

(**O-T**) Three days after tamoxifen treatment of $Tcf3^{GC/+}$; $ROSA26^{mTmG/+}$ mice, mGFP(+) *Tcf3*-lineage (*Tcf3* lin) cells are detected in the epithelia of the esophagus (O), tongue (Q), and plantar paw skin (S) (arrowheads) of tamoxifen-treated mice, but never in vehicle-treated control mice (P, R, T). Asterisks: autofluorescence of lingual filliform papillae. Scale bars: 50 μm (F-N); 100 μm (O-T).

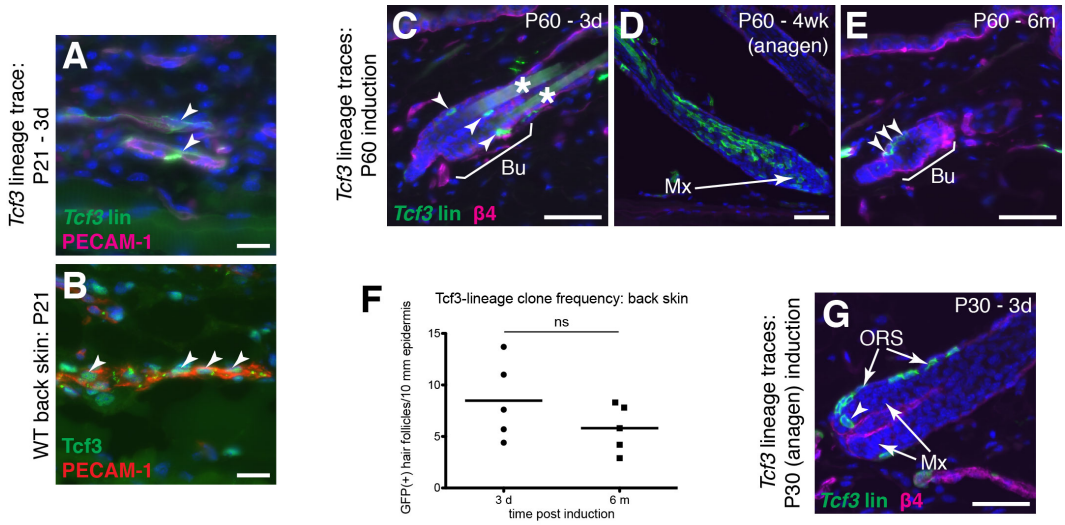

Figure S2. *Tcf3* labels hair follicle stem cells in adult skin.

(**A**, **B**) *Tcf3* is expressed in dermal blood vessels. (**A**) Colocalization of mGFP reporter (arrowheads) and endothelial marker PECAM-1 in *Tcf3*-lineage (*Tcf3* lin) dermal cells. (**B**) Antibody costaining for Tcf3 (arrowheads) and PECAM-1 verifies expression of *Tcf3* in dermal blood vessels.

(**C-E**) Lineage traces in $Tcf3^{GC/+}$; $ROSA26^{mTmG/+}$ mice with induction during the second postnatal telogen (~P60). Results are similar to those obtained with induction at P21. (**C**) Three days after induction, individual mGFP(+) cells (arrowheads) are observed within the hair follicle bulge (Bu). (**D**) In the subsequent anagen phase, mGFP(+) clones expand and incorporate into the growing hair shaft via the hair matrix (Mx). (**E**) Persistent clones (arrowheads), often multicellular, are still observed in the HF bulge (Bu) six months post induction.

(**F**) Quantitation of clone frequency in back skins three days and six months after induction of lineage tracing at P21/22. The majority (68.4 ± 3.7%, mean ± s.d.) of clones persist, with a moderate, non-significant decline in the frequency of labeled follicles (p =

0.42, Mann-Whitney *U* test). Dots represent number of labeled follicles per 10 mm dorsal skin in individual mice; bars indicate mean.

(**G**) Three days after lineage-tracing induction in anagen, *Tcf3*-lineage clones (arrowhead) are observed in transition between the outer root sheath (ORS) and the matrix (Mx) (compare Figure 1D, E).

Scale bars: 50 μm (all). Asterisks: hair shaft autofluorescence.

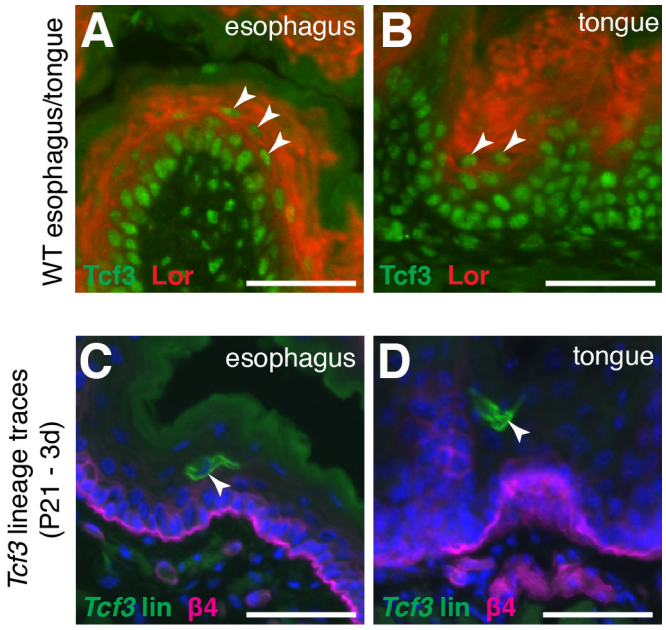

Figure S3. *Tcf3* expression is observed in differentiating suprabasal cells in esophageal and lingual mucosa.

(**A**, **B**) Immunofluorescent costaining for Tcf3 and granular layer marker loricrin (Lor) in esophageal (A) and lingual (B) mucosa. *Tcf3*-expressing cells (arrowheads) are observed within the differentiating granular layer.

(**C**, **D**) Three days after lineage-tracing induction, clones of solitary suprabasal *Tcf3*-lineage (*Tcf3* lin) cells (arrowheads) are seen in the esophagus (C) and tongue (D), confirming the specificity of Tcf3 antibody staining. β4: β4 integrin.

Scale bars: 50 μm.

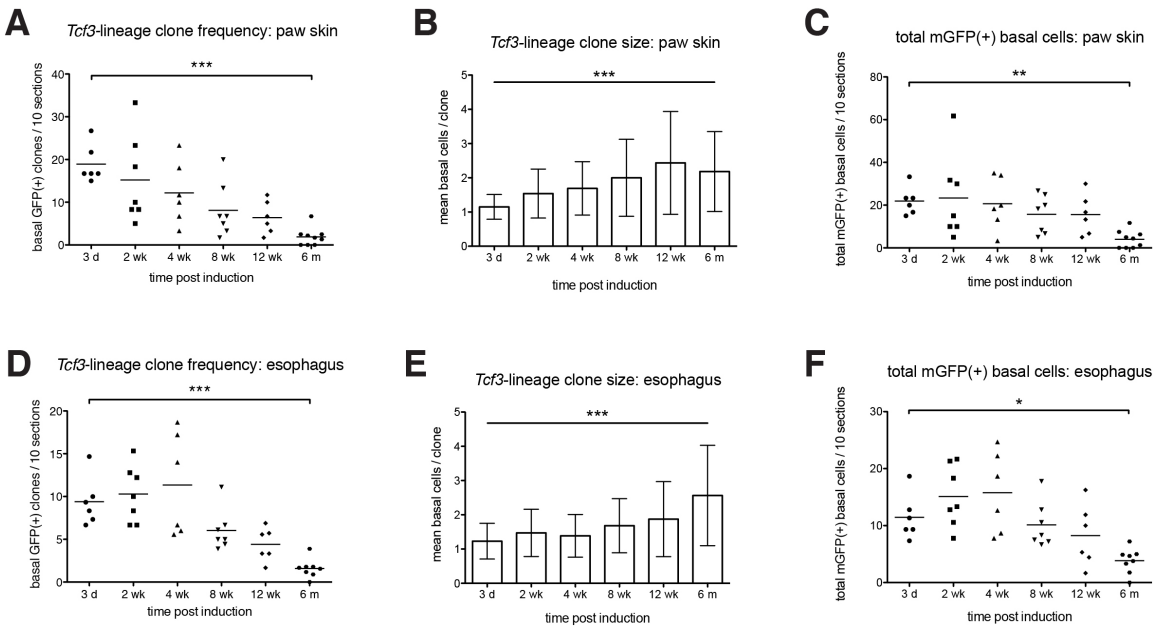

Figure S4. *Tcf3*-lineage clones are progressively lost over time in both paw skin and esophageal mucosa, and surviving clones expand laterally through the basal layer.

Tcf3$^{GC/+}$;*R26*$^{mTmG/+}$ mice were treated with tamoxifen at P21/22, and specimens of paw skin and esophageal mucosa were collected at various timepoints thereafter. The number of mGFP(+) clones (**A**, **D**), number of mGFP(+) basal cells per clone (**B**, **E**), and total number of mGFP(+) basal cells (**C**, **F**) were quantitated in random cryosections from both tissues. Counts were limited to those clones containing ≥ 1 basal cell in any given section.

(**A**, **D**) In both tissues, a progressive loss of clones was observed over time. Individual dots represent the number of mGFP(+) clones in individual mice, bars represent mean at each timepoint. Six months after induction, 9.9% ± 8.7% of initially labeled clones persisted in the paw skin; 17.0% ± 6.6% of clones persisted in esophagus (mean ± s.d., $p < 0.001$ for both comparisons, Dunn's multiple comparison test).

(**B**, **E**) Clone loss over time was accompanied by lateral expansion of the surviving clones through the basal layer. Columns represent the average number of basal cells per clone in all mice at each timepoint; error bars represent s.d. In both cases, the clone expansion over time was significant ($p < 0.0001$, Kruskal-Wallis test).

(**C**, **F**) The total number of labeled basal cells within both tissues declined over time, contrary to the predictions of the neutral competition model. However, the decrease only reached significance when comparing the 6-month and 3-day timepoints ($p < 0.01$ for both comparisons, Dunn's multiple comparison test).

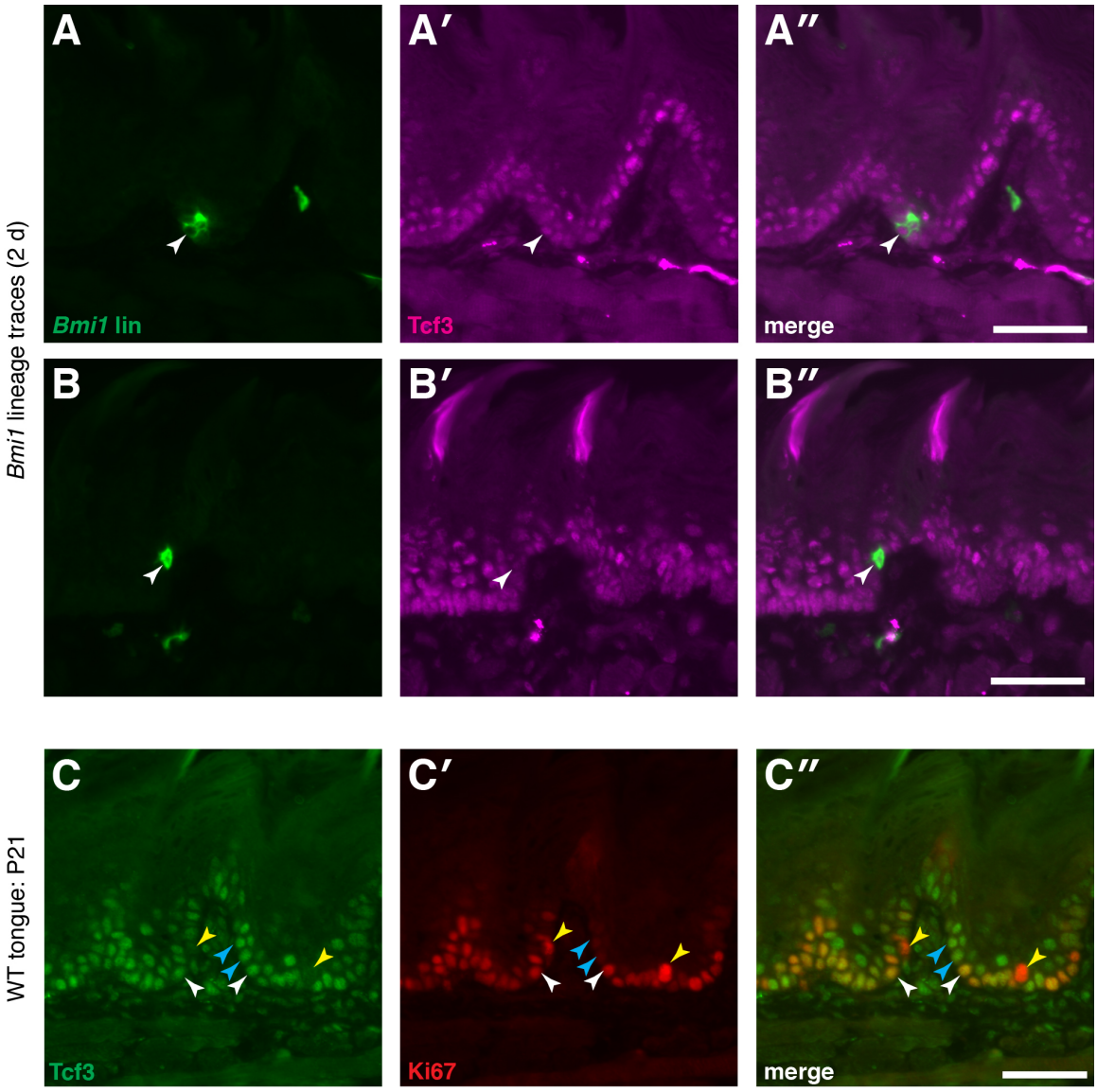

Figure S5. *Tcf3* expression does not correlate with *Bmi1* expression or proliferative status in the lingual epithelium.

(**A**, **B**) *Bmi1*$^{CreER/+}$;*R26*$^{mTmG/+}$ mice were treated with a single dose of tamoxifen and sacrificed two days later; specimens of tongue epithelium were collected and stained for Tcf3 protein. Clones of 1-2 *Bmi1*-lineage (*Bmi1* lin) basal cells (arrowheads) were observed at a frequency of ~1 cell/IPP, consistent with the previous report of Tanaka *et al*.

In some cases (**A**), the labeled cells expressed *Tcf3* at a level similar to that of neighboring cells; in others (**B**), they possessed little to no *Tcf3* expression. These observations suggest that expression of the two factors is not directly linked.

(**C**) Wild-type tongue specimens were costained for Tcf3 (green) and Ki67 (red) proteins. There was little correlation between expression of the two factors, and populations of cells were identified which were variously $Tcf3^{+}$ $Ki67^{+}$ (white arrowheads); $Tcf3^{+}$ $Ki67^{-}$ (blue arrowheads); and $Tcf3^{-}$ $Ki67^{+}$ (yellow arrowheads). These observations suggest that Tcf3 expression is not directly tied to proliferative status.

Scale bars: 50 μm (all).

Table S1. PCR primers for cloning, blotting and genotyping

Primer	Sequence (5’ → 3’)
GFP_T2A_fw	GGCTCTGGA GAGGGCAGAGGAAGTCTGCTAACATGCGGTGACGTCGAG GAGAATCCTGGCCCA ATGGTGAGCAAGGGCGAGG
GFP_F2A_rv	CCGCCAACTTGAGAAGGTCAAAATTCAAAGTCTGTTTCAC TCCGGATCC CTTGTACAGCTCGTCCATGCC
Cre_F2A_fw	CTTTGAATTTTGACCTTCTCAAGTTGGCGGGAGACGTGGA GTCCAACCCAGGGCCC ATGTCCAATTTACTGACCGTACAC
Cre_Nhe_Eco_rv	CCGAA GCTAGC GAATTC TCAAGCTGTGGCAGGGAAACC
T3KI_cass_fw	TCCCCGTGCTACAGGCCCAGCCTCTTTCCTTGGTCACCAA GTCTGCCCAC GGCTCTGGA GAGGGCAG
T3KI_cass_rv	ATCATTACTACTTGGAGTCCCGAGACAGCCTGCATAGAAC CGGGGGCAGC CGAAGTTATATTATGTACCTGACTGATG
PL253_genom_L2	ACCGAGTAGCTTCCTAGTTAGTCCTCTGTACTTGTTAGCT GTAGCAGCATAAGGTGAAAC GGCGCGCC GCGTCAGGTGGCACTTTTC
PL253_genom_R2	ACAAACAGATTCATTTACCAGTTCACTTCCTCTAGCAAGG CAGAGTCAACATTATAAAAT CCTGCAGG CTCTAGAGTCGAGCAGTGTGG
T3KI_5LR2_fw	AGCGAACGGGGTTGACCAGAGTGA
T3KI_5LR2_rv	AGCTCCTCGCCCTTGCTCACCATT
T3KI_3LR_fw	ATGCTTCTGTCCGTTTGCCGGTC
T3KI_3LR_rv	TCTAGTCCTGCACGGCTGGAAGTT
T3KI_5SB_fw	AGCGGAGCCCAGCTAAGTCGC
T3KI_5SB_rv	GGCTGCCCAGGAAATCACCCAA
T3KI_3SB_fw	GTATCACAGCTTTTCGGGGTTGCTC
T3KI_3SB_rv	CCTTCACATGTCTGTCCACTCACTG
Tcf3KI_fw	TCTGCTGACCTCTCCCCCTACT
Tcf3KI_GC_rv	AACTTGTGGCCGTTTACGTCGC
Tcf3KI_WT_rv	TGTGTTTCCCCCTTCCTCTCCT

Table S2. Antibodies used for immunofluorescence, immunohistochemistry and western blotting

Antibody	Manufacturer	Prod. No.	Dilution
rat anti-β4 integrin (CD104), clone 346-11A	BD Biosciences	553745	1:200 (IF)
rabbit anti-filaggrin	Covance	PRB-417P	1:500 (IF)
chicken anti-GFP	Abcam	ab13970	1:1,000 (IF)
rabbit anti-GFP	Life Technologies	A6455	1:500 (IF); 1:10,000 (IHC)
rabbit anti-keratin 1	Elaine Fuchs lab		1:500 (IF)
rabbit anti-keratin 5	Covance	PRB-160P	1:2,000 (IF)
rabbit anti-keratin 6	Elaine Fuchs lab		1:250 (IF)
rabbit anti-keratin 13, clone EPR3671	Abcam	ab92551	1:1,000 (IF)
mouse AE13 (anti-hair cortex cytokeratin)	Abcam	ab16113	1:100 (IF)
rabbit anti-Lef1, clone C12A5	Cell Signaling	2230	1:200 (IF)
rabbit anti-loricrin	Covance	PRB-145P	1:500 (IF)
rat anti-PECAM-1 (CD31), clone MEC 13.3	BD Biosciences	550274	1:100 (IF)
guinea pig anti-Tcf3	Nguyen lab		1:200 (IF; IHC w/ HIER); 1:1,000 (WB)
mouse AE15 (anti-trichohyalin)	Santa Cruz	sc-80607	1:100 (IF)
mouse anti-β-actin, clone AC-15	Sigma	A1978	1:50,000 (WB)

IF, immunofluorescence; IHC, immunohistochemistry; WB, western blot; HIER, heat-induced epitope retrieval (in 10 mM sodium citrate, pH 6.0)